COMITETUL DE STAT PENTRU ENERGIA NUCLEARĂ

INSTITUTUL CENTRAL DE FIZICĂ

[redacted]

BUCUREŞTI-MĂGURELE

ROMANIA

CENTRAL INSTITUTE OF PHYSICS
INSTITUTE FOR PHYSICS AND NUCLEAR ENGINEERING*
Bucharest, POB MG-6, ROMANIA

P.N.LEBEDEV PHYSICAL INSTITUTE**
ACADEMY OF SCIENCES, Moscow, USSR
and
JOINT INSTITUTE FOR NUCLEAR RESEARCH***
Dubna, Moscow region, USSR

IFIN -
FT-196-1980 October

Optimal sum-rule inequalities for spin 1/2 Compton scattering.III

L.V.Filkov**, I.Guiasu*, D.Pantea*,
E.E Radescu***+)

Abstract : The analyticity (optimal) bounds for proton Compton scattering presented in the preceding paper are herewith considered from the point of view of experimental tests. An essential function occuring in this new dispersion framework is constructed numerically making use of existing cross-section data above the pion photoproduction threshold. To secure a safer construction new measurements in the photon laboratory energy region 150 MeV-240 MeV and at small momentum transfers are necessary. The bounds on the scattering amplitudes in the low energy region below the pion photoproduction threshold are in general sufficiently restrictive so as to be useful in discriminating among variants of theoretical phenomenological analyses but subsequent extremizations needed in bounding only one combination of the amplitudes (the unpolarized differential cross-section) are weakening much the results. The question of strengthening the bounds by means of the combined use of analyticity and unitarity is discussed within a very crude example which nonetheless illustrates that the inclusion of the pion photoproduction data through more elaborate mathematical procedures would deserve the effort.

+) On leave of absence from the Central Institute of Physics, Bucharest, Romania.

1. INTRODUCTION

We are undertaking here a first attempt to materialize some newly developed dispersion methods by performing experimental tests for the analyticity (optimal) bounds on proton Compton scattering presented in refs /1/ and /2/ (hereafter called I and II respectively). Those bounds from the preceding paper (II) which involve only directly measurable quantities like the unpolarized differential cross-section (u.d.c.s.) will be confronted with data while those providing restrictions on the allowed values of the scattering amplitudes will be used as consistency checks for model calculations. Lately there has been renewed interest in the phenomenological dispersion theoretical study of the proton Compton effect (among recent analyses we mention refs./3/-/5/ and send the reader to the reviews /6/ and /7/ for information about the theoretical and experimental situation in this field). Model independent tests of such calculations may, in this context, prove helpful in reaching some clarifications about the assumptions or approximations used therein.

In Section II we construct an essential function of energy and momentum transfer $S(\nu^2,t)$ ($\nu = \frac{1}{4}(s-u)$, s,t,u = Mandelstam variables) which plays a central rôle in all the bounding procedures presently discussed. The construction is achieved by integration (at fixed momentum transfer) over the u.d.c.s. data above the pion photoproduction threshold; some interpolations or even rather crude parametrizations has to be adopted in order to cope with the lack of data in some kinematical regions. To improve the results obtained, new measurements are needed in the photon (laboratory)

energy region 150 MeV - 240 MeV and at momentum transfers squared less than 0.1 GeV^2 since this zone just above the inelastic threshold contributes largely to the integral.

Once the main goal, the construction of $S(\nu^2,t)$ was attained, the hierarchy of analyticity bounds for low energy proton Compton scattering, given in concrete form in II, is systematically pursued in the following Sections. In Section III, where only one interior ν^2-point, $\nu_B^2 = \frac{t^2}{16}$, is considered, an optimal sum-rule inequality (derived in I) relating a known function of t and of the proton anomalous magnetic moment to $S(\nu^2 = \nu_B^2, t)$ is subjected to experimental test. The bound is satisfied, but it appears rather weak. This weakness is to be attributed to the presence of unknown dynamical zeros in the analytic unitary amplitudes (a.u.a.)constructed in I and II.

Bounds arising from the consideration of two interior ν^2-points, ν_B^2 and a ν^2-value situated in the physical region but below the pion photoproduction threshold ν_o^2, are analyzed in Section IV. The optimal upper and lower bounds on the u.d.c.s. at $\nu^2 < \nu_o^2$ derived in the preceeding paper (II) in terms of the u.d.c.s. values above ν_o^2 and also in terms of the proton's anomalous magnetic moment, are checked numerically and, as already expected, turn out to be weak. As shown in Section V these bounds are only little strengthened if, giving up the full model independence, four out of the six Compton scattering amplitudes (those unaffected by the annihilation channel exchange contributions) are taken as reliably known from calculations based on fixed t unsubtracted dispersion relations.

Unlike the bounds on the cross-section, the original ones, restricting the domain of possible values of the scattering ampli-

tudes, are in general quite tight and become nearly saturated in the "three ν^2-points"-case examined in Section VI. The analyticity bounds on the scattering amplitudes at low energies are sufficiently strong to allow, as shown in Sections IV and VI, useful model independent tests of phenomenologic analyses, and possibly to discriminate among different variants. For illustration we have concentrated on the phenomenological dispersion treatment from ref./5/ which has been submitted to the checks provided by the optimal analyticity bounds of II. In Section VI the need of increasing correspondingly the accuracy in the determination of the function $S(\nu^2,t)$ when higher steps of the hierarchy of bounds are being used (i.e. when the number of the interior ν^2-points is gradually increased) is particularly stressed out.

In Section VII bounds involving derivatives of the a.u.a. at $\nu^2 = \nu_B^2$ are analyzed and model independent restrictions on the two delicate subtraction functions (of t) affecting the usual phenomenological dispersion approaches are numerically obtained. Unfortunately but, also, not unexpectedly, they are by an order of magnitude too weak to be practically useful.

The bounds analyzed until now rely only on (fixed - t) analyticity requirements (except s-u crossing and gauge invariance). The question of strengthening the inequalities through the additional use of the unitarity condition is discussed in Section VIII where it is shown, in the framework of a simple-minded semi-phenomenological approach that the inclusion of the pion-photoproduction data by means of an adequate mathematical treatment, albeit difficult, would be very promising. The last section (IX) is devoted to some short comments.

II. CALCULATION OF THE FUNCTION $S(\nu^2,t)$.

We have to compute

$$S(\nu^2,t) = \exp\left\{\frac{(\nu_o^2-\nu^2)}{2\pi}\int_{\nu_o^2}^{\infty} \frac{\ln\left[128\pi^2(m^2+2\nu'-\frac{t}{2})\left(\frac{d\sigma}{d\Omega}\right)_{c.m.}^{(\nu',t)}\right]d\nu'^2}{(\nu'^2-\nu^2)(\nu'^2-\nu_o^2)^{1/2}}\right\}, \quad (2.1)$$

$\nu = \frac{s-u}{4}$, $\quad s + t + u = 2m^2$

$\nu_o^2 = \left[\frac{1}{2}\mu(2m+\mu) + \frac{t}{4}\right]^2$, $\quad$ m = proton mass,

μ = pion mass ,

for certain physical t-values in the range

$$0 \geq t \geq t_o = -\left[\mu(2m+\mu)/(m+\mu)\right]^2 = -3.49\mu^2 \quad (2.2)$$

and for ν^2-values belonging to the interval from the threshold ν_{min}^2 of the considered reaction $\gamma p \to \gamma p$ to the theshold of the single pion photoproduction ν_o^2

$$\nu_{min}^2 \leq \nu^2 < \nu_o^2 \; ; \quad (2.3)$$

Also we shall need the values taken by $S(\nu^2,t)$ at the location of the s-r channel Born poles $\nu^2 = \nu_B^2 = \frac{t^2}{16}$, $S(\nu_B^2,t)$ which will enter all the inequalities we shall be dealing with.

Since most of the data are given at (laboratory) photon energy ω' and center of mass scattering angle θ'_c one has to organize the cross-section $\left(\frac{d\sigma}{d\Omega}\right)_{c.m.}$ from the integrand as a function of ν , t . We recall the kinematical relations :

$$\nu = m\omega + \frac{t}{4} , \qquad \nu' = m\omega' + \frac{t}{4} \quad ; \qquad (2.4)$$

$$\cos\theta_c = 1 + t\,\frac{1+\frac{2\omega}{m}}{2\omega^2} \quad , \quad \cos\theta_e = 1 + t\,\frac{1+2\frac{\omega'}{m}}{2\omega'^2}$$

The "prime" on kinematical variables evidentiates their relation with the integration variable ν'^2.

The integration over ν'^2 is considered separately in the following intervals (corresponding to ω' values) :

I. threshold integration region : 150 MeV < ω' <240 MeV ;

II. first resonance region: 240 MeV < ω' < 440 MeV;

III. resonance region: 440 MeV < ω' < 1100 MeV ;

IV. high energy region : ω' > 1100 MeV.

In order to avoid spurious complications at the lower integration limit ν_0^2 coming from the square root $(\nu'^2 - \nu_0^2)^{1/2}$ in the denominator of the integrand in Eq.(2.1), the function $S(\nu^2,t)$ and its particular case $S(\nu_B^2,t)$ were actually calculated, after changing the integration variable

$$\xi = \frac{1}{\mu^2}(\nu'^2 - \nu_0^2)^{1/2} \quad , \quad (\nu'/\mu^2) = [\xi^2 + (\nu_0/\mu^2)]^{1/2} \qquad (2.5)$$

and scaling the dimensional variables to the pion mass μ , from the expression

$$S(\nu^2,t) = \exp\left\{\frac{1}{\pi}\left[\left(\frac{\nu_B}{\mu^2}\right)^2 - \left(\frac{\nu}{\mu^2}\right)^2\right]^{1/2}\int_0^\infty d\xi\,\frac{\ell_n\left[0.632\cdot 10^{-3}\,\frac{d\bar\sigma}{d\Omega}\cdot\left(\frac{m_p^2}{\mu^2}+2\sqrt{\xi^2+\frac{\nu_0^2}{\mu^4}}-\frac{t}{2\mu^2}\right)\right]}{\xi^2+\frac{\nu_0^2}{\mu^4}-\frac{\nu^2}{\mu^4}}\right\} \qquad (2.6)$$

where

$$\frac{d\bar\sigma}{d\Omega} = \left(\frac{d\sigma}{d\Omega}\right)_{c.m.}\left(\sqrt{\xi^2\mu^4+\nu_0^2}\,,t\right)\cdot\frac{10^{32}}{cm^2}$$

(the bar over notations of cross-sections will have the same meaning, i.e. units of 10^{-32} cm^2, throughout this paper).

In region I the absence of data at the investigated points of t forces us to introduce theoretical value for $d\sigma/d\Omega$.

In region II (the $N^*(\frac{3}{2}, \frac{3}{2})$ resonance region) we use the experimental data of Genzel et al. /8/ synthetized by their fit formula

$$\left(\frac{d\bar{\sigma}}{d\Omega}\right)_{c.m.(fit)} = A(\omega') + B(\omega')\cos\theta'_c + C(\omega')\cos^2\theta'_c \qquad (2.7)$$

$A(\omega')$, $B(\omega')$, $C(\omega')$ are listed(in μb/sr) in Table 4 of ref./8/ for the ω' values $\omega' = 240, 280, 320, 360, 400$ MeV; they were obtained from a fit to the angular distributions (Table 3 of ref./8/) extracted from the results of the actual measurements (displayed in Table 2 of the same reference) complemented by forward differential cross-sections; the latter were computed by means of total γp cross-sections in conjuction with a certain single pion photoproduction phenomenological input. Eq.(2.7) can be written as

$$\left(\frac{d\bar{\sigma}}{d\Omega}\right)_{c.m.(fit)} = A_o(\omega') + B_o(\omega')\frac{t}{\mu^2} + C_o(\omega')\left(\frac{t}{\mu^2}\right)^2 \qquad (2.7')$$

and $\left(\frac{d\bar{\sigma}}{d\Omega}\right)_{c.m.(fit)}$ is further organized as a function of ρ,t with the aid of Eq.(2.5) and Eqs.(2.4) by smooth interpolation of the coefficients $A_o(\omega')$, $B_o(\omega')$, $C_o(\omega')$. For the reader's convenience, $A_o(\omega')$, $B_o(\omega')$, $C_o(\omega')$ are displayed in Table 1 (without error bars since anyway we are going to accept an overall corridor of variation of at least 10% on the cross-section figures used in the integrand). The first line of Table 1 contains the values of A_o, B_o, C_o

calculated from refs./4/, /5/. In the region I the coefficients A_o, B_o, C_o have been taken as straight lines joining the values at the points $\omega' = 150$ MeV and $\omega' = 240$ MeV. This procedure leads generally to an overestimation of the cross section with respect to the calculated values from ref./5/ (in both cases $F_\pi > 0$ and $F_\pi < 0$ considered there for the π^o -pole contribution in the t-channel).

The parametrization so obtained for $d\sigma/d\Omega$ works well only for $1.5\ \mu^2 < -t < 3.5\ \mu^2$ but will be used also even for very low values of (-t) (as low as $(-t) \sim 0.6\ \mu^2$), where in fact the lack of data compels us to rely merely on extrapolations rather than directly on experiment. We compare in Table 2, at $t=-0.6\ \mu^2$ $(\frac{d\bar{\sigma}}{d\Omega})_{c.m.(fit)}$ as calculated using Eq.(2.7') and the values of the coefficients given in Table 1, with the corresponding theoretical results $(d\bar{\sigma}/d\Omega)$(theory)from ref./5/ (the differences between the calculated cross-sections with $F_\pi > 0$ and those with $F_\pi < 0$ are negligible for $\theta'_c \lesssim 30^o$).

As seen from the Table 2 the differences between $(\frac{d\bar{\sigma}}{d\Omega})_{c.m.(fit)}$ and $(d\bar{\sigma}/d\Omega)$ (theory) are very small for 240 MeV $< \omega' <$ 320 MeV but become substantial for 320 MeV $< \omega <$ 440 MeV. However, it should not be forgotten that the comparison from the Table 2 illustrates the worst case ($t = -0.6\ \mu^2$) we are in and the figures from the last column represent, after all, calculated values.

In the IIIrd region (440 MeV $< \omega' <$ 1100 MeV) we use mainly the results obtained by M.Jung et al /9/ from measured angular distributions of proton Compton scattering at photon (laboratory) energies of 700, 750 and 800 MeV. The actual data

refer to center of mass angles of the scattered gamma ray ranging from 40° to 130°, corresponding to $(-t)$ values between 5 μ^2 and 37.5 μ^2, while we are really interested in $(-t)$ values less than 3.5 μ^2. So we shall again resort to extrapolations and use the parametrizations from figure 4 of ref./9/, obtained from the measured angular distributions together with calculated cross sections at 0° /10/, /11/ :

$$\left(\frac{d\sigma}{d\Omega}\right)_{c.m.} = \frac{1}{2\pi} \cdot \frac{(s'-m^2)^2}{2s'} \cdot \frac{d\sigma}{dt} = \frac{\omega'^2}{\pi\left(2\frac{\omega'}{m}+1\right)} \frac{d\sigma}{dt} =$$

$$= \left[\frac{\left(\frac{\omega'}{\pi}\right)^2}{\frac{2\omega'}{m}+1} \cdot \frac{(0.139)^2 \cdot 10^2 \cdot 4}{\pi} \left(10^{-32}\,\frac{cm^2}{}\right) \right] \cdot \begin{cases} e^{4.0\,t/GeV^2} & \text{for } \omega = 700\ MeV \\ e^{4.8\,t/GeV^2} & \text{for } \omega' = 750\ MeV \\ e^{5.0\,t/GeV^2} & \text{for } \omega' = 800\ MeV \end{cases} \quad (2.8)$$

This parametrization can be checked at the available values with the data displayed in fig.10 of ref./7/ and with the data of ref./12/ and is seen to agree, whenever the checks are possible, with the results from both these references. We hopefully use it for lower $(-t)$ values within the interval $0.6\ \mu^2 < -t < 3.5\ \mu^2$. For ω' in the intervals 440 MeV - 700 MeV , 700 MeV-750 MeV , 750 MeV-800 MeV rough smooth interpolations have been performed (for any t - value needed).

In the high energy region (IV) we rely on the review of Rollnik and Stichel /7/ and use for 4 GeV < ω' < 16 GeV the parametrization

$$\frac{d\sigma}{d\Omega} = \left(\frac{d\sigma}{d\Omega}\right)_0 e^{At + Bt^2}$$

where the extrapolated forward cross-section $(\frac{d\sigma}{dt})_o$ (decreasing from $\simeq$ 1 to 0.7 μb/GeV^2) and the (slowly) energy dependent coefficients A,B are taken over respectively from fig.12 and table 5 of ref./7/ (A $\simeq$ 5-8 GeV^{-2}; B is taken in general zero except for some points, e.g. B = 2.3 $\pm$ 0.5 GeV^{-4} at ω = 8 GeV and B = 1.7 $\pm$ 0.3 GeV^{-4} at ω' = 16 GeV). The values of $\frac{d\sigma}{dt}$ at 800 MeV and 4 GeV have been joined continuously through a straight line, the increasing kinematic factor $(\omega'/\mu)^2/[(2\omega'/m)+1]$ being kept variable. The integrals have been cut-off at 16 GeV.

Once the integrand has been specified as described above, a program has been devised for the calculation of the function $S(\nu^2,t)$ at the points ν^2 and t of interest. As a rule, preference has been given to overestimations in that intervals of the integration where the knowledge of the cross section was extremely poor, because, as already noted in II, all inequalities we are interested in remain valid if instead of $d\sigma/d\Omega$ one uses a quantity majorizing it. However, in order to avoid as much as possible the weakening of the bounds on the account of overestimations, we have refrained to increase artificially the integrand whenever we have thought there are reasonable hopes that the values put in for $d\sigma/d\Omega$ would eventually turn out to be close to the real situation. Our aim has been to calculate the function $S(\nu^2,t)$ as given by Eq.(2.1) and not a corresponding majorizing quantity, which would have been much easier; the obtained results, although perhaps, not yet fully reliable in view of the still incomplete experimental knowledge, should all the same be regarded as a first attempt in this direction.

The main contribution to the integration in the evaluation of the function $S(\nu^2,t)$ comes from the threshold region (1). This is illustrated in Table 3 in the case of $S(\nu_B^2,t)$; the order

of the relative contributions of the integration regions I, II, III, IV remains the same in $S(\nu^2,t)$. The entries represent calculated values of $S(\nu_B^2,t)$ at various values of t ($-t = 0.6\ \mu^2$, $1\mu^2$, $2\mu^2$, $3\mu^2$, $3.49\ \mu^2$) with the integration range restricted to domains of ω' - values corresponding to 150 MeV$<\omega'<$ 240 MeV, 150 MeV $< \omega' <$ 440 MeV, 150 MeV $< \omega' <$ 1100 MeV, 150 MeV$<\omega'<$ 16.000 MeV.

In Figure 1 the graphic of $S^2(\nu_B^2,t)$ is drawn and in table 4 the results of the calculation for $S(\nu_B^2,t)$ and $S(\nu^2,t)$ are given for some values of t (and ν^2) corresponding to (under the pion photoproduction threshold) photon (laboratory) energies ω and c.m. scattering angles θ_c of interest in the future analyses (the values chosen for ω, θ_c refer mainly to situations where experimental determinations of $d\sigma/d\Omega$ have been performed).

III. THE "ONE POINT" PROBLEM

In this Section we present the results of a numerical test of the sum rule inequality (6.6) of I written in an equivalent form in II (inequality (3.3) of this reference)

$$\sum_{i=1}^{6} \Phi_i^2(\nu_B^2,t) \leq S^2(\nu_B^2,t) \qquad (3.1)$$

The left hand side can be easily computed using Eqs.(2.31) of II, in terms of t and proton's charge and anomalous magnetic moment. In fig.2 the left hand side of the inequality (3.1) is represented as a function of t for $0 \leq -t \leq 3.49\ \mu^2$. As seen from Figs.1 and 2 the inequality (3.1) is satisfied but it appears to be very weak (by a factor ranging from 3 to 10 for $\frac{1}{4}(-t)$ varying from $0.6\ \mu^2$

to 3.49 μ^2). In Fig.3 both sides of the inequality (3.1) are drawn on a logarithmic plot. Since the inequality (3.1) is optimal, i.e. it can not be further improved under the same input, the appearing weakness is entirely of dynamic origin and somehow related to the (dynamic) real or complex interior zeros of the amplitudes ϕ_i. The weakness of the inequality (3.1) is not too astonishing taking into account the generality of the underlying hypotheses.

According to the inequality (3.1), the proton Compton scattering unpolarized differential cross-section above the pion photoproduction threshold implies by itself and on analyticity grounds alone a definite upper bound on the anomalous magnetic moment of the proton, $\varkappa$. In Table 5 we give $\sum_{i=1}^{6} \phi_i^2(\nu_B^2,t)$ calculated with $\varkappa$ taken as 1.793, 2.5, 3.6 and 5.4, and compare the results, for some values of t, with $S^2(\nu_B^2,t)$. The upper bound on $\varkappa$ appears so weak by a factor of 2-3 only.

The inequality (3.1) becomes stronger towards smaller values of (-t), but unfortunately this is also the direction in which the evaluation of $S(\nu_B^2,t)$ is less and less reliable in view of the scarce experimental information.

IV. THE "TWO POINTS" PROBLEM

We start considering numerical checks of the (optimal) bound on the u.d.c.s. $d\sigma/d\Omega$ at energies below the pion photoproduction threshold ($\nu_{min}^2 \leq \nu^2 < \nu_o^2$, $t_o \leq t \leq 0$), obtained in II in terms of the u.d.c.s. values above ν_o^2 and of the existing information at $\nu^2 = \nu_B^2$ (i.e. the knowledge of the proton's charge and anomalous magnetic moment).

According to Eqs.(3.49) of II one has to extremize

$$\frac{128\,\pi^2(2\nu-\frac{t}{2}+m^2)\frac{d\sigma}{d\Omega}}{S^2(\nu^2,t)} = \sum_{i=1}^{6} b_i \xi_i^2 \qquad (4.1)$$

with respect to the variables ξ_i subject to the restrictions (inequalities (3.51) of II) :

$$\begin{aligned} &1-\sum_{i=1}^{6}\xi_i^2 \geq 0 \quad , \\ &g\left(1-\sum_{i=1}^{6}\xi_i^2\right)-\left(1-\sum_{i=1}^{6}\xi_i\xi_i^\beta\right)^2 \geq 0 \quad , \end{aligned} \qquad (4.2)$$

where we have used the abbreviated notation

$$\begin{aligned} &\xi_i = \bar{\Psi}_i(\nu^2,t) \quad , \quad \xi_i^\beta = \bar{\Psi}_i(\nu_\beta^2,t) \quad , \\ &g = \frac{1}{1-x^2(\nu^2,t)}\left[1-\sum_{i=1}^{6}(\xi_i^\beta)^2\right] \end{aligned} \qquad (4.3)$$

The coefficients b_i are given by Eqs. (3.50), (3.45), (3.42), (3.43) of II, $x(\nu^2,t)$ by Eq.(3.9) of II and $\bar{\Psi}_i(\nu^2,t)$, $\bar{\Psi}_i(\nu_\beta^2,t)$ were introduced in Eqs.(3.46), (3.52) of II, respectively. The known coefficients ξ_i^β satisfy the inequality (3.1) which we rewrite as

$$1-\sum_{i=1}^{6}(\xi_i^\beta)^2 \geq 0 \; . \qquad (4.4)$$

The extremization has to be performed at any fixed pair of ν^2,t values of interest. One way of doing this extremization is to introduce two spurious variables ξ_7, ξ_8 in order to write the condition (4.2) as

$$1 - \sum_{i=1}^{6} \xi_i^2 - \xi_7^2 = 0 ,$$

$$g\left(1 - \sum_{i=1}^{6} \xi_i^2\right) - \left(1 - \sum_{i=1}^{6} \xi_i \xi_i^0\right)^2 - \xi_8^2 = 0 \qquad (4.5)$$

and look for the extremal values of $\sum_{i=1}^{6} b_i \xi_i^2$ employing two Lagrange multipliers ε, δ in connection with the first and, respectively the second of Eqs.(4.5). One arrives so at a system of 10 algebraic equations for ε, δ, ξ_7, ξ_8 and the values of ξ_i ($i = 1,2,\ldots 6$) realizing the extremum :

$$\begin{cases} b_k \xi_k + \varepsilon \xi_k + \delta g \xi_k - \delta \xi_k^0 \left(1 - \sum_{i=1}^{6} \xi_i \xi_i^0\right) = 0, \quad k = 1,2,\ldots,6 , \\ \varepsilon \xi_7 = 0 , \\ \delta \xi_8 = 0 , \\ \text{Eqs. (4.5)} . \end{cases} \qquad (4.6)$$

It is easy to verify using the inequality (4.4) that for $g < 1$ (as it will be actually the case in the numerical analysis below) only the solution with $\varepsilon = 0$, $\xi_8 = 0$ is of interest; this leads to the system

$$(b_k + \lambda)\,\xi_k = \lambda \xi_k^0 \frac{\sqrt{1-R^2}}{\sqrt{g}} , \quad k = 1,2,\ldots,6 , \qquad (4.7')$$

$$\sum_{i=1}^{6} \xi_i^2 = R^2 , \qquad (4.7'')$$

$$\sum_{i=1}^{6} \xi_i \xi_i^0 = 1 - \sqrt{g(1-R^2)} \qquad (4.7''')$$

where instead of ξ_7, δ, the new parameters λ, R^2 have been introduced as

$$\lambda = \delta_g \,, \qquad R^2 = 1-\xi_7^2 \,, \quad 0 \le R^2 \le 1 \,. \tag{4.8}$$

Solving for ξ_k (k=1,2,... 6) Eqs.(4.7) the following two equations for the two unknowns λ and R^2 are found :

$$\lambda^2 \sum_{i=1}^{6} \frac{(\xi_i^0)^2}{(\ell_i+\lambda)^2} = \frac{R^2 g}{1-R^2} \,,$$

$$\lambda \sum_{i=1}^{6} \frac{(\xi_i^0)^2}{(\ell_i+\lambda)} = g\left[\frac{1}{\sqrt{g(1-R^2)}} - 1\right] \,. \tag{4.9}$$

R^2 may be further eliminated and a complicated algebraic equation for λ is obtained.

Returning to Eqs.(4.7'), (4.1) one can find so the desired maximum and minimum values of $\frac{d\sigma}{d\Omega}$, $(\frac{d\sigma}{d\Omega})_{max(min)}$. The extremization has been actually carried out on a computer.

As seen from Eqs. (4.7"), (4.7'") in the process of extremization, the region of interest in the ξ_i- space is determined by the intersection between the sphere (4.7") of radius R and the plane (4.7'"). The condition that the distance $d(R^2)$ from the origin to the plane (4.7'" be smaller or equal to R (which also excluded before the + sign in front of the square root $\sqrt{g(1-R^2)}$ in Eq.(4.7'")) is

$$d^2(R^2) = \frac{\left[1-\sqrt{g(1-R^2)}\right]^2}{\sum_{i=1}^{6} (\xi_i^0)^2} \le R^2 \tag{4.10}$$

and restricts R^2 to the interval

$$1 - y_-^2 \leq R^2 \leq 1 - y_+^2 \tag{4.11}$$

where

$$y_\pm = \frac{\left[1-x^2(\nu^2,t)\right]\sqrt{g}}{1 \pm x^2(\nu^2,t)\left[\sum_{i=1}^{6}(\xi_i^B)^2\right]^{1/2}} \tag{4.12}$$

λ and R^2 have been varied so as to fulfil Eqs.(4.9) and numerical results for $(d\sigma/d\Omega)_{max}$ and $(d\sigma/d\Omega)_{min}$ were finally obtained. $(d\sigma/d\Omega)_{max(min)}$ are displayed for several cases of ω, θ_c in columns 2 and 3 of Table 6 where the existing corresponding experimental values (column 7) as well as the results(column 6) of the phenomenological calculations of ref. /5/ (for both alternatives $F_\pi > 0$ and $F_\pi < 0$ regarding the π^0 - exchange in the t-channel) are listed.

As seen from Table 6, the knowledge of $d\sigma/d\Omega$ above the pion photoproduction threshold ν_o^2 and the knowledge of the proton anomalous magnetic moment, although establish precise upper and lower bounds on the permissible values of $d\sigma/d\Omega$ below ν_o^2, are not sufficient to put more stringent restrictions on the unpolarized cross-section. However, the situation within the two points problem is not as bad from a practical point of view as it may seem judgind only from the bounds on $d\sigma/d\Omega$. Indeed, the restrictions (4.2) referring to the amplitudes directly, are very tight as it may be seen from Table 7 in the same cases of ω, θ_c as those considered in Table 6 for $d\sigma/d\Omega$. Calculated values of the

amplitudes from ref. /5/ were introduced (again in both alternatives $F_\pi > 0$, $F_\pi < 0$) in the ineqs. (4.2). The inequalities appear satisfied in all cases but nearly saturated. As seen from Table 7, the inequalities (4.2) give rise to no violation and so we can not exclude, within the "two points" problem, the alternative $F_\pi < 0$, even though in this case inequalities (4.2) are nearer to saturation than in the case $F_\pi > 0$. The fact that the bounds on $d\sigma/d\Omega$ are confortably large as against the ones very stringent on the amplitudes is entirely understandable in view of the subsequent extremization which has to be performed in going from six amplitudes to a single combination of them, $d\sigma/d\Omega$.

Within the "two points" problem, the conclusion therefore is that the optimal bounds provided by our formalism are not strong enough for distinguishing between disputable (low energy) experimental determinations of $d\sigma/d\Omega$ on fully model independent grounds, but are practically helpful in testing phenomenological calculations of the scattering amplitudes which have to survive the checks imposed by inequalities (4.2).

V. BOUNDS ON $d\sigma/d\Omega$ OBTAINED BY ENLARGING THE INPUT

Since the bound on the low energy values of $d\sigma/d\Omega$ discussed within the "two points" problem in Section IV turned out to be too weak for practical aims, we have tried to obtain an analogous stronger inequality by enlarging the information one is starting with on account of some abandonments of the full model independence. Four out of the six Bardeen-Tung invariant amplitudes for proton Compton scattering (A_3, A_4, A_5 and A_6 in

the notations of ref. /5/) will be taken as known (from ref./5/) as they can be quite reliably calculated by means of unsubtracted fixed-t dispersion relations in terms of single pion photoproduction data. Then ξ_i, $i=1,4,5,6$ in Eq.(4.1) become fixed and known quantities and the lower and upper bounds on $d\sigma/d\Omega$, denoted by $(d\sigma/d\Omega)^{o}_{min}$, $(d\sigma/d\Omega)^{o}_{max}$ are found by looking for an extremum of $\xi_2^2 + \xi_3^2$ (we recall that the coefficients of ξ_2^2 and ξ_3^2 in Eq. (4.1) are equal : $b_2 = b_3$) with the restrictions (see ineq. (4.2)) :

$$\begin{aligned} &\xi_2^2 + \xi_3^2 = r^2 \leq 1 - \Delta_1 \quad , \\ &g(1 - \Delta_1 - r^2) \geq (1 - \xi_2^{o}\xi_2 - \xi_3^{o}\xi_3 - \Delta_2)^2 \quad , \\ &\Delta_1 = \sum_{i=1,4,5,6} \xi_i^2 \quad , \\ &\Delta_2 = \sum_{i=1,4,5,6} \xi_i^{o}\xi_i \quad . \end{aligned} \tag{5.1}$$

Denoting

$$B(r^2) = 1 - \Delta_2 - \left[g(1 - \Delta_1 - r^2)\right]^{1/2} \tag{5.2}$$

the extremal values of r^2 are furnished by the equation

$$r^2 = \frac{B^2(r^2)}{(\xi_2^B)^2 + (\xi_3^B)^2} \quad , \qquad 0 \leq r^2 \leq 1 - \Delta_1 \tag{5.3}$$

which has always two real positive solutions if $1-\Delta_2-\left[g(1-\Delta_1)\right]^{1/2} < 0$ (this condition is fulfilled in all cases numerically analyzed below). So one finds the desired maximum, r^2_{max}, while the

(absolute) minimum is $r^2_{min} = 0$, i.e. $\xi_2 = \xi_3 = 0$. If one looks into the expression of the amplitudes ϕ_i in terms of $\bar{A}_i(\nu^2,t)$ (Eqs. (2.21), (2.23) of II), one sees that $(d\sigma/d\Omega)^o_{min}$ is thereby obtained by calculating it with the two amplitudes $\bar{A}_1(\nu^2,t)$, $\bar{A}_2(\nu^2,t)$ (affected by annihilation channel contributions) taken as

$$\bar{A}_1^{(o)}(\nu^2,t) = \frac{4\nu^2}{m^2(4m^2-t)}\,\bar{A}_3(\nu^2,t)$$

$$\bar{A}_2^{(o)}(\nu^2,t) \equiv \frac{4\nu^2}{m^2 t}\,\bar{A}_3(\nu^2,t) \quad , \qquad (5.4)$$

$$(\nu^2_{min} \leq \nu^2 < \nu^2_o \;\; ; \;\; 0 < (-t) \leq (-t_o)\;).$$

$(d\sigma/d\Omega)^o_{min}$ is so no longer dependent on the S-function. $(d\sigma/d\Omega)^o_{max(min)}$ were so calculated using the numerical values for A_3, A_4, A_5, A_6 from ref. /5/ and the results at some energies and angles of interest are displayed for comparison in columns 4 and 5 of Table 6.

The improvement over $(d\sigma/d\Omega)_{max(min)}$ calculated previously in Section IV is seen to be minor in spite of the heavy price paid for it by fixing in a reliable but not entirely model independent way four out of the six amplitudes describing the process. On the other side, however, this rather unsuccessful attempt to strengther more significantly the bounds on $d\sigma/d\Omega$, may be regarded as an almost model independent confirmation of the important rôle played by the amplitudes A_1, A_2 at low energies,

established other wise only qualitatively by arguments based on the existing low energy theorems. Since in the framework of the procedure used in this Section the place left to the t-channel contributions (*enterring through the amplitudes* A_1, A_2) still remains unexpectedly large, other analogous stronger bounds should be looked for in order to achieve a more precise understanding of the real influence of the physics in the annihilation channel on the low energy proton Compton scattering.

VI. THE "THREE POINTS" PROBLEM

The hierarchy of restrictions on the amplitudes $\phi_l(\nu^2,t)$ ($l = 1,2,\ldots 6$) provided by the formalism developed in I and II leads to stronger and stronger bounds when the number of the considered interior points gradually increases. We shall deal here with the amplitudes $\phi_l(\nu^2,t)$ taken at $\nu^2 = \nu_B^2$ and at two other interior points $\nu_{min}^2 \leq \nu_1^2$, $\nu_2^2 < \nu_o^2$ ($t_o \leq t \leq 0$) and shall submit the phenomenological calculation of the Compton scattering amplitudes from ref /5/ to the test furnished by the bound (3.29) of II specified to the case of three interior points (p=3). The non-negativity conditions of the 3x3 matrix

$$G_{(p=3)} \equiv \begin{vmatrix} \dfrac{1-\sum_{l=1}^{6}(\xi_l^{(1)})^2}{1-x_1^2} & ; \; 1-\sum_{l=1}^{6}\xi_l^{(1)}\xi_l^{0} & ; \; \dfrac{1-\sum_{l=1}^{6}\xi_l^{(1)}\xi_l^{(2)}}{1-x_1x_2} \\ 1-\sum_{l=1}^{6}\xi_l^{(1)}\xi_l^{0} & ; \; 1-\sum_{l=1}^{6}(\xi_l^{0})^2 & ; \; 1-\sum_{l=1}^{6}\xi_l^{(2)}\xi_l^{0} \\ \dfrac{1-\sum_{l=1}^{6}\xi_l^{(1)}\xi_l^{(2)}}{1-x_1x_2} & ; \; 1-\sum_{l=1}^{6}\xi_l^{(2)}\xi_l^{0} & ; \; \dfrac{1-\sum_{l=1}^{6}(\xi_l^{(2)})^2}{1-x_2^2} \end{vmatrix} \geq 0 \qquad (6.1)$$

where

$$\xi_i^{(1),(2),0} = \bar{\psi}_i\,(\nu^2_{1,2,0}\,,t)\quad, \tag{6.2}$$

$$X_{1,2} = \frac{(\nu_o^2-\nu_0^2)^{1/2} - (\nu_o^2-\nu_{1,2}^2)^{1/2}}{(\nu_o^2-\nu_0^2)^{1/2} + (\nu_o^2-\nu_{1,2}^2)^{1/2}}\quad, \tag{6.3}$$

lead, for instance, to

$$1 \geq G_j \geq 0\quad,\qquad j = 1,2,3 \tag{6.4}$$

with

$$G_1 \equiv \sum_{i=1}^{6} (\xi_i^{(1)})^2\quad, \tag{6.5}$$

$$G_2 = \frac{\left[1-\sum_{i=1}^{6}\xi_i^{(1)}\xi_i^{0}\right]^2(1-X_1^2)}{\left[1-\sum_{i=1}^{6}(\xi_i^{(1)})^2\right]\left[1-\sum_{i=1}^{6}(\xi_i^{0})^2\right]}\quad, \tag{6.6}$$

$$G_3 = \left\{\frac{\left[1-\sum_{i=1}^{6}\xi_i^{(2)}\xi_i^{0}\right]^2\left[1-\sum_{i=1}^{6}(\xi_i^{(1)})^2\right]}{1-X_2^2} + \frac{\left[1-\sum_{i=1}^{6}\xi_i^{(2)}\xi_i^{0}\right]^2\left[1-\sum_{i=1}^{6}(\xi_i^{(1)})^2\right]}{1-X_1^2}\right\}\cdot$$

$$\cdot\left\{\left[1-\sum_{i=1}^{6}(\xi_i^{0})^2\right]\left|\frac{\left[1-\sum_{i=1}^{6}(\xi_i^{(1)})^2\right]\left[1-\sum_{i=1}^{6}(\xi_i^{(2)})^2\right]}{(1-X_1^2)(1-X_2^2)} - \frac{\left[1-\sum_{i=1}^{6}\xi_i^{(1)}\xi_i^{(2)}\right]^2}{(1-X_1X_2)^2}\right| + \right.$$

$$\left. + \frac{2\left[1-\sum_{i=1}^{6}\xi_i^{(1)}\xi_i^{0}\right]\left[1-\sum_{i=1}^{6}\xi_i^{(2)}\xi_i^{0}\right]\left[1-\sum_{i=1}^{6}\xi_i^{(1)}\xi_i^{(2)}\right]}{1-X_1X_2}\right\}^{-1} \tag{6.7}$$

The function $S(\nu^2,t)$ being determined at $\nu^2 = \nu_B^2$, $\nu^2 = \nu_1^2$, $\nu^2 = \nu_2^2$ as described in Section II and using for the Compton scattering amplitudes entering $\xi_l^{(1),(2)}$ $(l=1,2,\ldots 6)$ the results of ref./5/ in both alternatives $F_\pi > 0$ and $F_\pi < 0$ we have computed the quantities $G_{1,2,3}$ which should satisfy the restrictions (6.4). The results are displayed (for some value of t) in the Table 8. The corridors of variation in $G_{1,2,3}$ have been roughly estimated by letting all $S(\nu_B^2,t)$, $S(\nu_1^2,t)$, $S(\nu_2^2,t)$ vary with an (exagerated) amount of $\pm$ 10% (this corresponds roughly to an accepted $\pm$20% variation of $d\sigma/d\Omega$ from the integrand). As seen from the Table 8, the calculation of ref./5/ survives the strong test imposed by the bounds (6.4) but only in the alternative $F_\pi > 0$ for the sign of the $\pi^0 \to \gamma\gamma$ coupling. The violation $G_3 > 1$ obtained for $F_\pi < 0$ in the case $t = -3\mu^2$ ($\nu_1 = 5.93\ \mu^2$, $\nu_2 = 6.43\ \mu^2$; the physical threshold of the process corresponds to $\nu_{min} = 5.87\ \mu^2$ while the pion photoproduction threshold is $\nu_0 = 6.47\ \mu^2$) illustrates the practical usefulness of the bounding procedure envisaged here in discriminating among different variants of the phenomenological dispersion approaches to the proton Compton effect.

Looking in turn at the figures for G_1, G_2 and G_3 from the Table 8 one may realize how the "one", "two" and "three points" bounds put progresively stronger and stronger demands upon the scattering amplitudes (things were so arranged as to have the proximity to 1 taken for reference). A warning, however, is necessary. The pretentions on the level of precision in the evaluation of the function $S(\nu^2,t)$ become higher and higher in proportion

as the number of the considered interior points increases (this is understandable since one is dealing with analytic objects). In this respect, due to the sensitivity of $S(\nu^2,t)$ upon the threshold integration zone, new measurements of the unpolarized differential cross-section in the energy region arround the pion photoproduction threshold (and at $(-t) < 3.5\ \mu^2$) are badly needed in order to improve the accuracy in the construction of this essential function.

We end this Section by mentioning that the restrictions (6.4) on the amplitudes may, through extremization procedures similar to the one used in Section IV, be turned into correlations (expressed by inequalities) among the allowed values of the unpolarized differential cross section at two different (under the pion-photoproduction threshold) points ν_1 and ν_2. Such bounds relating directly measurable quantities should warrant investigation but we shall not pursue it here.

IV. BOUNDS INVOLVING DERIVATIVES AT $\nu^2 = \nu_B^2$

In this Section we shall present numerical evaluations for some bounds on $\left.\frac{\partial \phi_{2,3}(\nu^2,t)}{\partial \nu^2}\right|_{\nu^2=\nu_B^2}$ resulting from certain particular cases of the inequalities (3.28) of II. The input information is represented by the knowledge of $\frac{d\sigma}{d\Omega}(\nu,t)$ above ν_o^2 and the values of $\phi_i(\nu^2,t)$, $(i=1,2,\ldots 6)$ at $\nu^2 = \nu_B^2$ as given by Eqs.(2.31) of II. Such bounds on $\left.\frac{\partial \phi_{2,3}(\nu^2,t)}{\partial \nu^2}\right|_{\nu^2=\nu_B^2}$ are, in principle, interesting since they provide analyticity constraints on the two highly model dependent subtraction functions $F_1(t)$ and

$F_2(t)$ affecting two of the invariant amplitudes in the usual dispersion theoretical calculations of the proton Compton effect at low and intermediate energies /4/, /5/. We write the dispersion representation for the Bardeen-Tung invariant amplitudes $A_i(\nu,t) \equiv A_i^{Born}(\nu,t) + A_i^c(\nu,t)$, $(i=1,2,\dots 6)$ from ref. /5/ as

$$A_1^c(\nu,t) = F_1(t) - k_1 \frac{t}{\pi} \int_{(m+\mu)^2}^{\infty} \frac{A_3^{(s)}(s',t)\, ds'}{(s'-m^2+t)(s'-m^2)} - \tag{7.1}$$

$$- \frac{(t^2-16\nu^2)}{2\pi} \int_{(m+\mu)^2}^{\infty} \frac{(s'-m^2+\frac{t}{2})\, A_i^{(s)}(s',t)\, ds'}{(s'-m^2)(s'-m^2+t)\left[(s'-m^2+\frac{t}{2})^2-4\nu^2\right]} ,$$

$$(i=1,2), \quad k_1 = 1, \quad k_2 = -\frac{1}{m} ,$$

$$A_{3,6}^c(\nu,t) = \frac{4\nu}{\pi} \int_{(m+\mu)^2}^{\infty} \frac{A_{3,6}^{(s)}(s',t)\, ds'}{\left[(s'-m^2+\frac{t}{2})^2-4\nu^2\right]} , \tag{7.2}$$

$$A_{4,5}^c(\nu,t) = \frac{2}{\pi} \int_{(m+\mu)^2}^{\infty} \frac{(s'-m^2+\frac{t}{2})\, A_{4,5}^{(s)}(s',t)\, ds'}{\left[(s'-m^2+\frac{t}{2})^2-4\nu^2\right]} \tag{7.3}$$

The superscript (s) denotes the s-channel absorptive parts of the amplitudes. The identification of the subtraction functions $F_{1,2}(t)$ is

$$F_1(t) = (A_1^c - A_3^c)(u=m^2,t) = A_1^c(\nu_B^2,t) + t\, a_3(t) , \tag{7.4}$$

$$F_2(t) = (A_2^c + \frac{1}{m} A_3^c)(u=m^2,t) = A_2^c(\nu_B^2,t) - \frac{t}{m} a_3(t) \qquad (7.5)$$

$$a_3(t) \equiv \frac{1}{\pi} \int_{(m+\mu)^2}^{\infty} \frac{A_b^{(a)}(\nu',t)\, d\nu'}{(\nu'^2-m^2)(\nu'^2-m^2+t)} \quad , \qquad (7.6)$$

and their model calculation relies usually on dispersion relations in the t-variable. We note that

$$F_1(t=0) = 4\pi\,(\alpha - \beta) \qquad (7.7)$$

where α and β are respectively the (generalized) electric and magnetic polarizabilities of the proton while $F_2(t)$ contains the π^0 (t-channel) pole

$$F_2(t) = \frac{2}{m} \frac{F_\pi g_{\pi NN}}{\mu^2 - t} + \text{higher that single particle dispersion contributions}$$

$$\equiv F_2^{(\pi^0\text{-pole})}(t) + F_2^{\text{correction}}(t). \qquad (7.8)$$

F_π is the $\pi^0 \to \gamma\gamma$ decay constant and $g_{\pi NN}$ the strong πNN coupling constant. $F_\pi \cdot g_{\pi NN} > 0$ (as it should have been written in the 10th line from the bottom on the page 302 of ref /5/) corresponds to the $N\bar{N}$ model calculation of the $\pi^0 \to \gamma\gamma$ decay and is also the sign which seems to be favored by the Primakoff effect.

Specializing the inequalities (3.28) of II to the case in which only one derivative

$$\xi_2' \equiv 4(\nu_0^2 - \nu_0^2)\left.\frac{d\xi_2}{d\nu^2}\right|_{\nu^2 = \nu_0^2} \tag{7.9}$$

is considered, one has the restrictions

$$\begin{aligned} &1 - \sum_{i=1}^{6} (\xi_i^0)^2 - (\xi_2')^2 \geq 0 \quad , \\ &\left[1 - \sum_{i=1}^{6} (\xi_i^0)^2 - (\xi_2')^2\right]\left[1 - (\xi_2^0)^2\right] - (\xi_2^0)^2 (\xi_2')^2 \geq 0 \quad . \end{aligned} \tag{7.10}$$

(We note that the inequalities (3.28) of II hold as they stand only for the analytic amplitudes ψ_i , but $\bar{\psi}_i = \psi_i$ for i=1,2,3,5 and only $\bar{\psi}_{4,6}$ are non-analytic (unitary) combinations of $\psi_{4,6}$ according to Eqs (3.46) of II). One can easily show that the inequalities (7.10) lead to the constraint

$$-\sqrt{G_0} \leq \xi_2' \leq +\sqrt{G_0} \tag{7.11}$$

where

$$G_0 = \left[1 - \sum_{i=1}^{6} (\xi_i^0)^2\right]\left[1 - (\xi_2^0)^2\right] \tag{7.12}$$

Now, since

$$\xi_2' = 4(\nu_0^2 - \nu_0^2)\left[\frac{\left.\frac{\partial \Phi_2(\nu^2,t)}{\partial \nu^2}\right|_{\nu^2=\nu_0^2}}{S(\nu_0^2,t)} - \frac{\left.\frac{\partial S(\nu^2,t)}{\partial \nu^2}\right|_{\nu^2=\nu_0^2}}{S(\nu_0^2,t)} \cdot \xi_2^0\right] \tag{7.13}$$

and

$$\begin{aligned} \left.\frac{\partial \Phi_2}{\partial \nu^2}\right|_{\nu^2=\nu_0^2} = \frac{1}{4(\nu_0^2 - \nu_0^2)}\Bigg\{ &2\Phi_2(\nu_0^2,t) - \frac{e^2(2\varkappa + \varkappa^2)t}{\sqrt{2}\, m (4m^2 - t)^{1/2}} - \\ &- \frac{t(4m^2-t)^{1/2}}{2\sqrt{2}} F_1(t) + \frac{4m^2 t^2}{2\sqrt{2}(4m^2-t)^{1/2}} a_3(t) \Bigg\} , \end{aligned} \tag{7.14}$$

one finally arrives at the bound

$$W_2(t) \leq \left[\mu^3 F_1(t)\right] + \frac{4m^2}{4m^2 - t}\left(-\frac{t}{\mu^2}\right)\mu^5 a_3(t) \leq W_1(t) . \qquad (7.15)$$

$W_{1,2}(t)$ are known (model independent) functions of t, determined by $\varkappa$ and the values taken by $\frac{d\sigma}{d\Omega}(\nu,t)$ above the pion photoproduction threshold ν_o^2 ($\frac{d\sigma}{d\Omega}$ enters, this time, not only through the function $S(\nu_B^2,t)$ but through $\left.\frac{\partial S(\nu^2,t)}{\partial \nu^2}\right|_{\nu^2=\nu_B^2}$ as well). The quantity $\mu^5 a_3(t)$ may be reliably calculated (starting from Eq. (7.6) in terms of photoproduction data and turns out to be very small ($\sim 10^{-4}$) compared with W_1, W_2 and with model calculations of $\mu^3 F_1(t)$. As seen from the Table 9 the bound (7.15) for $(-t) = (2 \div 3)\mu^2$ is by an order of magnitude too weak, which otherwise is not so unexpected taking into account the fact that the real input information is more or less the same as the one underlying the weak result from Section III. Towards smaller values (-t) the bound becomes weaker and weaker since for $(-t) \to 0$, $W_{1,2} \to \pm \infty$ like $\mp \frac{(const>0)}{t}$ as it should (in the forward direction the amplitude $A_1(\nu,t)$ disappears from the expression of $\frac{d\sigma}{d\Omega}$). The same arguments applied in connection with

$$\xi_3' \equiv 4(\vartheta^2 - \vartheta_o^2)\left.\frac{d\xi_3}{d\vartheta^2}\right|_{\vartheta^2=\vartheta_o^2} \qquad (7.16)$$

lead to an analogous bound

$$-\sqrt{H_o} \leq \xi_3' \leq +\sqrt{H_o} \qquad (7.17)$$

involving the second subtraction function $F_2(t)$. The expression of H_o is obtained from that of G_o Eq.(7.12) through the obvious

replacement of the index 2 by 3. Using

$$\left.\frac{\partial \Phi_3(\vartheta^2,t)}{\partial \vartheta^2}\right|_{\vartheta^2=\vartheta_0^2} = \frac{1}{4(\vartheta_0^2-\vartheta_0^2)}\left\{2\Phi_3(\vartheta_0^2,t) + \right.$$

$$\left. + \frac{m(-t)^{1/2}}{2\sqrt{2}}\left[\frac{2e^2}{m^2}(2\varkappa+\varkappa^2) + t F_2(t)\right]\right\} \tag{7.18}$$

and a formula analogous to Eq.(7.13), one ends with

$$w_2(t) \leq -\mu^4 F_2(t) \leq w_1(t) \tag{7.19}$$

where $w_{1,2}(t)$ are again known, model independent, functions of t (for $(-t) \to 0$, $w_{1,2}(t)$ behave like $\pm$ (const > 0)$(-t)^{-3/2}$). Numerical tests of the bound (7.19) are presented in the Table 10 for $(-t) = 2\mu^2$ and $(-t) = 3\mu^2$. Its weakness is roughly the same as that of the bound expressed by the inequalities (7.15) and prevents drawing a clear-cut conclusions about the sign of F_π within the information which was accepted as known here.

The bounds derived in this Section, notwithstanding their sad weakness, represent rigorous analyticity restrictions on the two important unreliable subtraction functions occuring in the usual dispersion theory of the proton Compton effect. By enlarging the input information, especially through the inclusion of photoproduction data by means of the unitarity condition, one may hope that such bounds could be gradually strengthened up to a more convenient level.

VIII. SEMIPHENOMENOLOGIC BOUNDS ON $d\sigma/d\Omega$.

As seen from Sections IV. and V the optimal lower and upper bounds on $\frac{d\sigma}{d\Omega}$ at low energies hitherto obtained in a model inde-

pendent way in Section IV and in an almost model independent way in Section V, are not enough stringent to be practically useful in challenging some of the existing experimental points. The information one was starting with appears so insufficient to lead through analyticity alone to stronger constraints on $\frac{d\sigma}{d\Omega}$ and therefore it has tc be further enlarged. A natural way of doing this is to appeal to the consequences of the unitarity condition and, for instance specify, (over the portion of the cut from its beginning up to the threshold for double pion photoproduction), the imaginary parts of the six invariant amplitudes of the Compton effect in terms of data on single pion photoproduction.

Obtaining optimal bounds under such an enlargement of the input raises, however, difficult mathematical problems. Under a particular limited but precise formulation of the starting information, definite results can be obtained notwithstanding mathematical and computational obstacles. Work in this direction is in progress and the results will be reported elsewhere. For the time being, in this Section we shall examine within a simple semiphenomenologic approach what may be gained from the inclusion of the photoproduction data.

The usual dispersion theoretical studies (to the lowest order in el ctromagnetism) of the proton Compton effect at low and intermediate energies rely firstly on certain general assumptions underlying the dispersion representation adopted and then on approximations and models for the calculation of the needed adsorptive parts of the amplitudes, in various channels. Among the most recent analyses we mention those of Refs. /3/,/4/,

/5/, /12/. The rather well extracted pion photoproduction multipoles establish the s-channel absorptive parts of the Compton invariant amplitude over a sufficiently large energy range and represent the main input information in such calculations. The strongest model dependence occurs in connection with the scarcely known annihilation channel contributions affecting those two of the six amplitudes describing the process, (A_1 and A_2 in the notations used in /5/) for which the expected high energy behaviour at fixed momentum transfer (as given, for instance, by the normal Regge-pole model), is not sufficient to write down unsubtracted dispersion relations (u.d.r.). So eventually one has to deal with two unpleasant (subtraction) functions of t, usually further evaluated by dispersing in t and using more or less reliable approximations to handle the appearing annihilation channel absorptive parts.

The question of the rôle played by the annihilation channel exchange in proton Compton scattering in general, as well as particularly in the study of the electromagnetic polarizabilities of the proton which determine the process at very low (i.e. substantially under the first inelastic threshold) energies, is a problem interesting per se and has been already either touched upon or considered in detail by various authors /15/-/21/, /5/, /4/. The main efforts were directed to lower, on the account of the annihilation channel exchanges, the theoretical prediction for the unpolarized differential cross-section at energies under the pion photoproduction threshold, in order to achieve a closer agreement with data. The needed t-channel absorptive parts of the $\gamma p \to \gamma p$ process in the two particle unitarity approximations are

determined by the amplitudes of the reactions $pp \to \pi\pi$ and $\pi\pi \to \gamma\gamma$; the largest uncertainities were related to the latter. The simple model for the $\pi\pi \to \gamma\gamma$ amplitude devised in Refs /19/, /5/ as well as the corresponding analyses of refs /20/, /22/, which all furnish results not too far away from the Born-pole approximation (i.e. from the pure quantum electrodynamics (QED) result for $\pi\pi \to \gamma\gamma$) seem to agree with recent measurements at PLUTO, DESY /23/ of $\sigma_{\gamma^*\gamma^* \to 2}$ mesons which comes out close to the QED prediction. The $\pi\pi \to \gamma\gamma$ calculation of ref./24/ gave for $\sigma_{\gamma\gamma \to \pi\pi}$ exceedingly large values compared with $\sigma^{QED}_{\gamma\gamma \to \pi\pi}$, but in view of the existing (polynomial) ambiguities in fixing the amplitude, it seems that even this calculation could accommodate solutions near to the Born-poles approximation.

Here we shall not pursue the line of building models or approximation schemes for the needed poorly known amplitudes but, instead, shall adopt the opposite point of view and try to bring some clarifications on the size of the annihilation channel contributions by bounding them more or less rigorously, in order to see as clearly as possible what place is really left for model constructions. The bound to be next presented is very simple minded and rather semi-phenomenological in nature than rigorous; is consist in the extremization (at every fixed energy and scattering angle values of interest) of the unpolarized differential cross-section (which is a positive definite bilinear form in the amplitudes) with respect to the two real parts of those amplitudes affected by subtractions. All the six imaginary parts are considered as known (according to the unitarity condition) in terms of pion photoproduction data and the other four real parts

are also taken as known quantities being evaluated through u.d.r. as integrals over their imaginary parts. Strictly speaking, the imaginary parts are only approximately known and so are the four real parts computed from the u.d.r., whereby the incertaintles are even larger.

However, all these approximations are exactly the same as in the standard treatments and therefore the obtained bounds although not rigorous and hence not entirely satisfactory in direct confrontation with data, will, at least, clearly say that once some specified approximations were adopted, the unpolarized differential cross-section can not be any longer lowered below a certain explicitly found minimum value, irrespective of any ability in deriving models for the annihilation channel exchanges.

A safer but weaker bound which nevertheless proved itself useful in clarifying discrepancies between single pion photoproduction multipole analysis and Compton scattering data in the N^* (1236 MeV) resonance region was firstly put forward in ref./3/. It exploited the fact that the actual u.d.c.s. should be always larger than the u.d.c.s. calculated with all the six real parts of the amplitudes set equal to zero and used only the unitarity to fix the imaginary parts. Unlike this purely unitarity bound, the one we are going to present relies in addition on analyticity, although in a very crude and naive way.

For definiteness we shall work in the context of the dispersion analysis of ref./5/ and use the same notations, amplitudes and conventions.

The fixed -t dispersion representation for the $A_i(\nu,t)$ ($i= 3,4,5,6$) is that from Eqs.(7.2) and (7.3).

Extremizing (at (ν,t) fixed) the expression of $(\frac{d\sigma}{d\Omega})_{c.m.}$ as a bilinear form in $A_1(\nu,t)$ (Eq.(2.12) of ref./5/) with respect to A_1, A_2 ($A_{3,4,5,6}$ are kept fixed) the semiphenomenologic lower bound is found

$$(\frac{d\sigma}{d\Omega}) \geq (\frac{d\sigma}{d\Omega})^{(ph.)} \tag{8.1}$$

where the right hand side is calculated taking for ReA_1, ReA_2 the following expressions

$$(Re\ A_1)^{(ph.)} = \frac{4\nu}{(4m^2 - t)} Re\ A_3 , \tag{8.2}$$

$$(Re\ A_2)^{(ph.)} = \frac{4\nu}{mt} Re\ A_3$$

$Re\ A_3 = A_3^{Born} + Re\ A_3^c$ as well as $Re\ A_{3,4,5,6}$ are established in terms of pion photoproduction data according to Eq.(7.2) and (7.3) and of their known nucleon Born poles A_l^{Born}, $(l=3,4,5,6)$. Unlike the rest of this paper, the bound (8.1) is not restricted to (ν^2,t) values within the intervals $\nu^2_{min} \leq \nu^2 < \nu_o^2, 0 \leq -t \leq -t_o$ but applies to all angles in the laboratory energy region from threshold up to well beyond the $N^*(\frac{3}{2}, \frac{3}{2})$ resonance tail.

The results of the calculation of $(\frac{d\sigma}{d\Omega})^{(ph.)}$ (performed using $Im\ A_l$, $(l=1,2,\ldots 6)$ and $Re\ A_l$ $(l=3,4,5,6)$ from ref./5/) are drawn in Figs. 4-15 (dotted line) together with the purely unitarity bound

$$\frac{d\sigma}{d\Omega} \geq (\frac{d\sigma}{d\Omega})_{ReA_l=0,\ (l=1,2,\ldots 6)} \tag{8.3}$$

(dashed-dotted line) and the calculated $\frac{d\sigma}{d\Omega}$ from ref./5/ in both cases for F_π ($F_\pi > 0$ dashed line and $F_\pi < 0$ solid line). The legenda of the experimental points in Figs.4-15 is the same as in the corresponding figures of ref./5/; the black triangles oriented upwards ▲ indicate data taken from ref./8/.

The bound (8.1) is substantially stronger than the purely unitarity bound; it leads to some violations (especially in the N^* resonance region) which cast some doubts either on the extraction of the single pion-photoproduction multipoles employed or on the involved experimental values of $\frac{d\sigma}{d\Omega}$ themselves. Although very crude and approximate, the inequality (8.1) represents an analyticity and unitarity bound and suggests that the inclusion of the photoproduction input by means of more intelligent methods than a pure algebraic extremization would deserve the effort.

IX. SOME COMMENTS

In this paper, the bounding methods developed in refs. /1/, /25/, /2/ on the basis of mathematical procedures aimed to achieve a maximal exploitation of the fixed momentum transfer analyticity properties of the Compton scattering amplitudes to the lowest order in the fine-structure constant, have been considered from the point of view of the confrontation with data. A crucial stage in checking the bounds was the construction (accomplished in Section II) of the function $S(\nu^2,t)$ by means of the existing experimental values of the proton Compton scattering unpolarized differential cross-section above the pion photoproduction threshold. We did do it as well as we could, which does not mean at all that no space for real improvement has been left. The work

reported here being a first attempt to test the bounds, in some places we have certainly oversimplified the treatment, willing s we were to see before long how the whole apparatus does work. The possible uncertainties did not seem to matter much in as far as the restrictions belonging to the first steps of the considered hierarchy of bounds turned out to be weak, but soon (more precisely within the "three points" problem) the special need for serious control on the approximations involved in the construction of the S-function became manifest. The bounds refered to the scattering amplitudes directly and not to some combinations of them like the differential cross-section, are really strong already when a single ν^2-interior point except ν_B^2 is considered and become nearly saturated when an additional interio: point is included (Section VI). They are therefore indeed useful as model independent tests of the phenomenological calculations of the proton Compton effect at low energies. In order to draw safe conclusions when the number of the ν^2-interior points is increased, one has to know to a corresponding degree of accuracy the S-function. To achieve this, new measurements of the differential cross-section in the kinematical region 150 MeV < ω < 240 MeV, $(-t) < 3.5\ \mu^2$, which is practically the region of formation of the S-function are necessary. Measurements at higher energies but smaller angles than up to now considered (such that $(-t) < 3.5\ \mu^2$) would also be desirable in this respect.

In the framework of what we have named the "two points" problem the analyticity bounds on the low energy cross-section (Section IV) are satisfied but they are disapointingly weak as

regards their possible utility in discriminating among controversial experimental results. This weakness which can be traced back to the sum rule inequality analyzed in Section III (the "one point" problem) is to be attributed (because of the optimality of the bounds) to the presence of dynamical zeros in the analytic unitary amplitudes introduced in refs. /1/, /2/ and may, perhaps, turned into an advantage in phenomenological treatments as it allows new types of economic parametrizations.

The optimal inequalities commented so far were established starting exclusively from analyticity requirements. The primitive approach from Section VIII illustrates, we hope, that the question of strengthening the bounds through the combined use of analyticity and unitarity by means of more decent techniques, is worthy of further investigation.

Table 1. Values of the coefficients $A_o(\omega')$, $B_o(\omega')$, $C_o(\omega')$.

ω' (MeV)	$A_o(\omega')$	$B_o(\omega')$	$C_o(\omega')$
150	0.00	- 0.90	- 0.090
240	6.10	0.56	0.083
280	18.50	2.58	0.248
320	36.20	5.06	0.340
360	24.70	2.46	0.143
400	17.80	1.66	0.081
440	11.90	0.69	0.030

Table 2. Comparison between $(\frac{d\bar{\sigma}}{d\Omega})_{c.m.(fit)}$ and $(\frac{d\bar{\sigma}}{d\Omega})_{(theory)}$ (ref./5/) (as the bar on σ indicates, the figures refer to units of 10^{-32} cm^2); $t = -0.6\ \mu^2$.

ω'(MeV)	θ'_c	$(\frac{d\sigma}{d\Omega})_{c.m.(fit)}$	$(\frac{d\sigma}{d\Omega})_{(theory)}$ ref./5/
240	32.3°	5.8	6.0
280	28.3°	17.0	17.5
320	25.4°	33.2	29.0
360	23.1°	23.3	30.0
400	21.3°	16.8	23.0
440	19.7°	11.5	20.0

Table 3. $S(\nu_B^2, t)$ calculated (for the specified values of t) with the integration restricted over the regions (I), (I+II), (I+II+III), (I+II+III+IV).

Integration restricted to \ $\frac{(-t)}{\mu^2}$	0.6	1	2	3	3.49
$150 \leq \omega'(\text{MeV}) \leq 240$	0.423	0.446	0.480	0.497	0.501
$150 \leq \omega'(\text{MeV}) \leq 440$	0.416	0.438	0.467	0.480	0.484
$150 \leq \omega'(\text{MeV}) \leq 1100$	0.419	0.439	0.466	0.478	0.480
$150 \leq \omega'(\text{MeV}) \leq 16000$	0.459	0.480	0.506	0.515	0.516

Table 4. $S(\nu_B^2,t)$ and $S(\nu^2,t)$ calculated at some particular values of the photon lab. energy ω and c.m. scattering angle θ_c.

ω MeV	θ_c	$-t/\mu^2$	ν/μ^2	ν_o/μ^2	ν_{min}/μ^2	$S(\nu_B^2,t)$	$S(\nu^2,t)$
	30°	0.044	2.879	7.212	0.704	0.385	0.358
	60°	0.164	2.849	7.182	1.361	0.414	0.388
60	90°	0.328	2.808	7.141	1.926	0.436	0.411
	120°	0.492	2.767	7.100	2.391	0.452	0.428
	150°	0.612	2.737	7.07	2.633	0.460	0.437
	30°	0.107	4.646	7.196	1.101	0.402	0.326
	60°	0.400	4.572	7.123	2.129	0.443	0.370
97	90°	0.801	4.472	7.023	3.014	0.471	0.403
	120°	1.201	4.372	6.923	3.696	0.488	0.433
	150°	1.494	4.299	6.849	4.125	0.496	0.436
80.9	94.60°	0.619	3.742	7.068	2.649	0.460	0.415
85.4	94.70°	0.685	3.942	7.051	2.788	0.464	0.414
109.9	95.60°	1.103	5.018	6.947	3.541	0.484	0.395
86.3	152.20°	1.217	3.853	6.918	3.721	0.488	0.441
106.7	152.60°	1.798	4.690	6.773	4.529	0.503	0.429
111.1	152.60°	1.935	4.868	6.739	4.701	0.505	0.424

Table 5. $\sum_{i=1}^{6} \phi_i^2(\nu_B^2,t)$ calculated with several test values for $\mathcal{K}$ and compared with $S^2(\nu_B^2,t)$.

t/μ^2	$\sum_{i=1}^{6} \phi_i^2(\nu_B^2,t)$ calculated with :				$S^2(\nu_B^2,t)$
	$\mathcal{K}=1.793$	$\mathcal{K}=2.5$	$\mathcal{K}=3.6$	$\mathcal{K}=5.4$	
0.175	0.085	0.133	0.353	1.503	0.173
0.875	0.076	0.127	0.336	1.380	0.225
1.400	0.070	0.120	0.316	1.263	0.244
2.480	0.053	0.095	0.248	0.938	0.262
3.490	0.022	0.040	0.097	0.333	0.266

Table 6. Numerical results for the upper and lower bounds on $\frac{d\sigma}{d\Omega}$ (units of 10^{-32} cm^2 everywhere) at several values of the photon lab.energy ω (MeV) and c.m. scattering angle θ_c. The columns 2 and 3 refer to the bounds discussed in Section IV while the columns 4 and 5 to the bounds obtained in Section V by enlarging the imput information. For reference, corresponding theoretical and experimental results for $\frac{d\sigma}{d\Omega}$ are listed in the columns 6 and 7 respectively. The corridors of variation indicated, for illustration, only in the first line, correspond to an accepted $\pm$ 10% change in $\frac{d\sigma}{d\Omega}$ used in the integrands of $S(\nu^2,t)$ and $S(\nu_B^2,t)$.

ω (MeV) θ_c t	$(\frac{d\sigma}{d\Omega})_{max}$	$(\frac{d\sigma}{d\Omega})_{min}$	$(\frac{d\sigma}{d\Omega})^{o}_{max}$	$(\frac{d\sigma}{d\Omega})^{o}_{min}$	$(\frac{d\sigma}{d\Omega})$ (ref/5/) (theory)	$(\frac{d\sigma}{d\Omega})$ (exp)
80.9 94.6° $t=-0.62\mu^2$	6.78$\pm$ 0.67	0.42$\mp$ 0.10	4.82$\pm$ 0.70	0.55	($F_\pi>0$)1.09 ($F_\pi<0$)1.19	1.16$\pm$0.06 ref./13/
109.9 95.6° $t=-1.10\mu^2$	5.07	0.26	4.17	0.56	($F_\pi>0$)1.13 ($F_\pi<0$)1.37	1.03$\pm$0.06 ref./13/
97 150° $t=-1.49\mu^2$	8.61	0.03	7.12	0.07	($F_\pi>0$)1.89 ($F_\pi<0$)2.34	2.57$\pm$0.51 (θ_c=138.7°) ref./14/
111.10 152.6° $t=-1.94\mu^2$	7.76	0.02	6.46	0.07	($F_\pi>0$)2.0 ($F_\pi<0$)2.65	1.70$\pm$0.07 ref./13/

Table 7. Numerical tests of the Compton scattering amplitudes calculated in ref./5/ against the inequalities (4.2) so organized as the figures in the 3rd and 4th columns compare to 1. The label "(theory)" indicates that the ξ_i (i=1,2,...,6) in the corresponding expressions have been computed using the phenomenological results from ref./5/. The corridors of variation in the last column correspond to an overall 20% increase and decrease of the actual integrand used in the calculation of the function $S(\nu^2,t)$ (which leads to a change of some ±10% in $S(\nu^2,t)$ itself).

ω (MeV) θ_c	sign of F_π	$\left(\sum_{i=1}^{6} \xi_i^2\right)_{\text{theory}}$	$\left\{\frac{\left[1-\sum_{i=1}^{6} \xi_i \xi_i^B\right]^2}{9\left[1-\sum_{i=1}^{6} \xi_i^2\right]}\right\}_{\text{theory}}$
80.9 95°	$F_\pi > 0$ $F_\pi < 0$	0.382 0.382	0.996 ± 0.001 0.996 ± 0.001
109.9 95.6°	$F_\pi > 0$ $F_\pi < 0$	0.328 0.330	0.977 ± 0.005 0.979 ± 0.005
97 150°	$F_\pi > 0$ $F_\pi < 0$	0.286 0.287	0.985 ± 0.002 0.991 ± 0.002
111.1 152.6°	$F_\pi > 0$ $F_\pi < 0$	0.259 0.263	0.978 ± 0.005 0.982 ± 0.005

Table 8. Numerical tests of the proton Compton scattering amplitudes calculated in ref. /5/ against the inequalities (6.4).

$-t/\mu^2$	ν_1/μ^2 ω_1 (MeV) $\vartheta_{c,1}$	ν_2/μ^2 ω_2 (MeV) $\vartheta_{c,2}$	G_1	G_2	G_3	F_π
1	3.73 82.6 132.9°	6.57 141.6 68.4°	0.316±0.045	0.995±0.001	1.000±0.001	$F_\pi>0$
			0.316±0.074	0.995±0.001	1.000±0.001	$F_\pi<0$
2	4.97 113.6 151.2°	6.49 145.1 102.2°	0.256±0.060	0.975±0.004	0.999±0.001	$F_\pi>0$
			0.261±0.061	0.980±0.006	1.000±0.001	$F_\pi<0$
3	5.93 138.6 166.1°	6.43 149.0 137.3°	0.269±0.065	0.907±0.031	1.004±0.010	$F_\pi>0$
			0.327±0.078	0.976±0.062	1.025±0.010	$F_\pi<0$

Table 9. Calculated values of $W_1(t)$ and $W_2(t)$ for some values of t. In the second column the corresponding results of the model calculation of $\mu^3 F_1(t)$ from ref./5/ are listed.

$-t/\mu^2$	$\mu^3 F_1(t)$	$\frac{-4m^2 t}{4m^2-t}\mu^3 a_3$	$W_2(t)$	$W_1(t)$
2	0.0032	-0.0001	-0.036	0.056
3	0.0029	-0.0002	-0.022	0.043

Table 10. Calculated values of $w_1(t)$ and $w_2(t)$ for some values of t. In the third column the corresponding results of the model calculation of $-\mu^4 F_2^{\text{correction}}$ from ref./5/ are listed. The upper and lower signs in the second column correspond respectively to $F_\pi > 0$ and $F_\pi < 0$.

$-t/\mu^2$	$-\mu^4 F_2^{\pi^0\text{-pole}}(t)$	$-\mu^4 F_2^{\text{correction}}(t)$	$w_2(t)$	$w_1(t)$
2	$\mp$ 0.0048	0.0008	-0.0813	0.0500
3	$\mp$ 0.0036	0.0009	-0.0508	0.0258

REFERENCES

1. I.Guiaşu, E.E.Rădescu and I.Raszillier, Optimal sum-rule inequalities for spin 1/2 Compton scattering, Central Institute of Physics, Bucharest, Report FT-184-1979, Annals of Physics(N.Y) 127, 436 (1980) (herein called I).
2. I.Guiaşu and E.E.Rădescu, Optimal sum-rule inequalities for spin 1/2 Compton scattering II (preceding article) (herein called II).
3. W.Pfeil, H.Rollnik and S.Stankowski, Nucl.Phys.B73, 166 (1974).
4. D.M.Akhmedov and L.V.Filkov, Nucl.Phys. B 125, 530 (1977); Yadernaya Fizika 25, 1021 (1977).
5. I.Guiaşu, C.Pomponiu and E.E.Rădescu, Annals of Physics (N.Y.), 114, 296 (1978).
6. P.S.Baranov and L.V.Filkov, Fizika Elem.Chastits I Atomnogo Yadra 7, 108 (1976).
7. H.Rollnik and P.Stichel, Springer Tracts in Modern Physics, 79, 1 (1977).
8. H.Genzel, M.Jung, R.Wedermeyer and H.J.Weyer, Zeitschrift für Physik, A 279, 399 (1976)
9. M.Jung, J.Kattein, H.Kuck, P.Leu, L.D.de Marné, R.Wedemeyer and N.Wermes, Bonn University Report HE-77-17 (1977) (submitted to the 1977 Int.Symp.on lepton and photon Inern.at High En., Hamburg).
10. T.A.Armstrong et al., Phys.Rev. D5, 1640 (1972).
11. H.Genzel, Bonn.Univ. PIB-1-153 (1972) (quoted in ref.9).
12. K.Toshioka et al., Nucl.Phys. B141, 364 (1978)
13. P.Baranov et al., Phys.Letters, B52, 122 (1974).
    P.Baranov et al., Zh.Eksperim. Teor.Fiz.Lett., 19, 777 (1974)

14. B.B.Govorkov et al., Dokl.Akad.Nauk USSR 3, 988 (1956).

15. A.C.Hearn and E.Leader, Phys.Rev. 126, 789 (1962).

16. D.Holliday, Ann.Phys. (N.Y.), 24, 289 (1963); 24, 319 (1963).

17. R.Köberle, Phys.Rev. 166, 1558 (1968)

18. T.E.P.Ericson, CERN Report TH/2021 ; "Interaction Studies in Nuclei" (H.Joachim and B.Ziegler, Eds.), p.577, North-Holland, Amsterdam, 1975.

19. I.Gulaşu and E.E.Rădescu, Phys.Rev. D18, 1728 (1978)

20. D.M.Akhmedov and L.V.Filkov, Lebedev Phys.Inst.Report No.232 (1978).

21. V.M.Budnev and V.A.Karnakov, Yadernaya Fizika, 30, 440 (1979)

22. V.M.Budnev, A.N.Vall and V.V.Serebryakov, Yadernaya Fizika 21, 1033 (1975)

23. W.Wagner, DESY Report 79/49 August 1979.

24. O.Babelon, J.L.Basdevant, D.Caillerie, M.Gourdin and G.Mennessier, Nucl.Phys. B144, 252 (1976)

25. I.Raszillier, Revue Roumaine de Physique, 24, 873 (1979); Central Institute of Physics, Bucharest, Reports FT-161-1978; FT-165-1979; FT-170-1979.

FIGURE CAPTIONS

Fig.1. The t-dependence of $S^2(\nu_B^2,t)$

Fig.2. The t-dependence of $\sum_{i=1}^{6} \phi_i^2 (\nu_B^2,t)$

Fig.3. The t-dependence of $\ln \sum_{i=1}^{6} \phi_i^2 (\nu_B^2,t)$ and of $\ln S^2(\nu_B^2,t)$.

Fig.4-15 Experimental data for the c.m. unpolarized differential cross-section at various photon lab.energies ω and c.m. scattering angles θ_c compared with the semi-phenomenological bound (8.1) (dotted line), purely unitarity bound (8.3) (dashed-dotted line) and the theoretical results from ref./5/ ($F_\pi > 0$ dashed line and $F_\pi < 0$ - solid line). The experimental points are marked in ref. /5/; black triangles oriented upwards ▲ represent points taken from ref./8/.

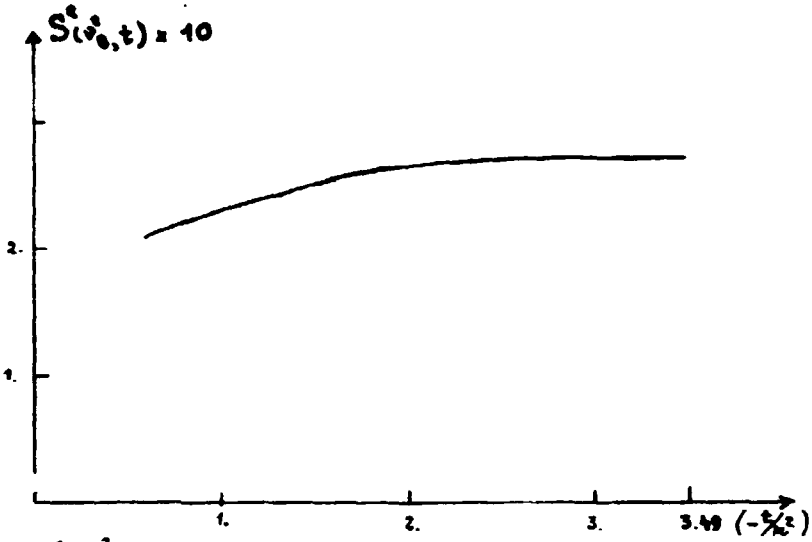

Fig.1.

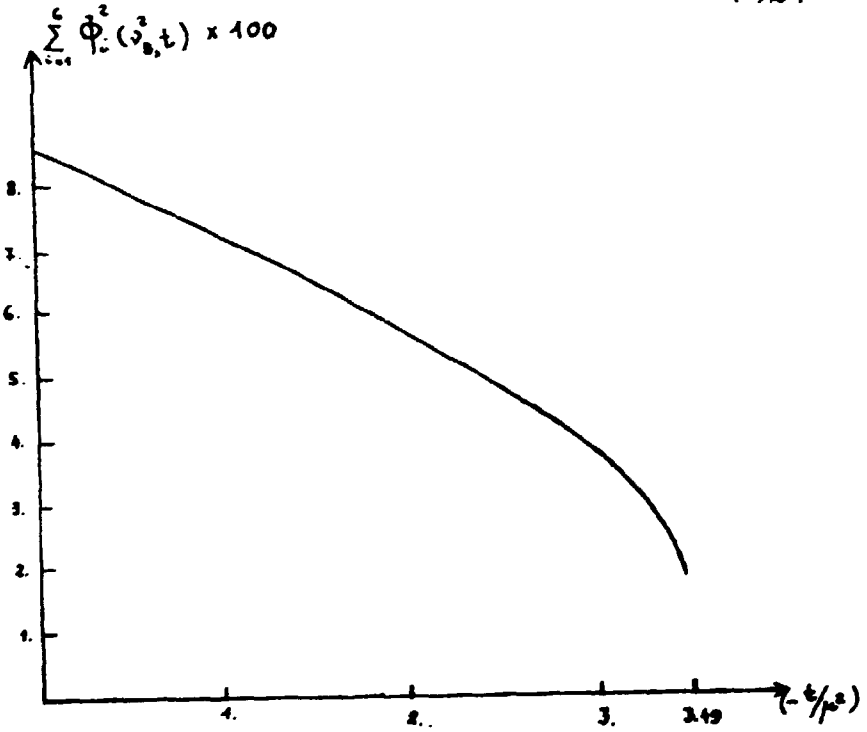

Fig.2.

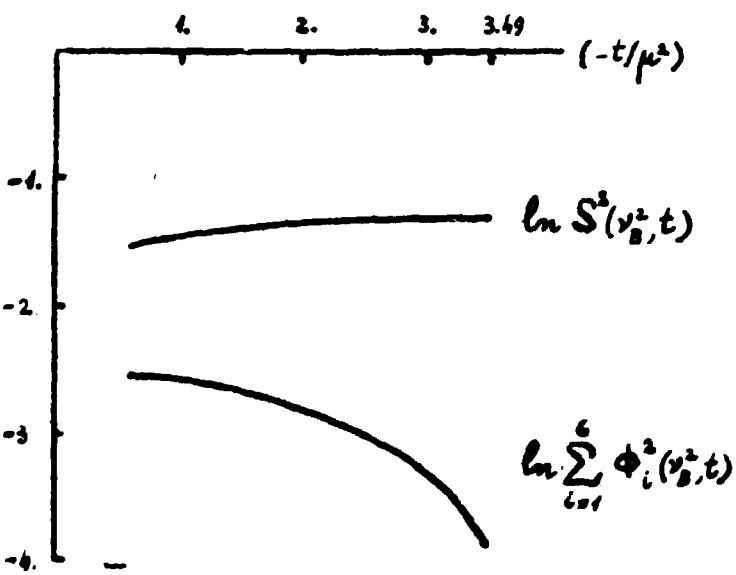

Fig.3.

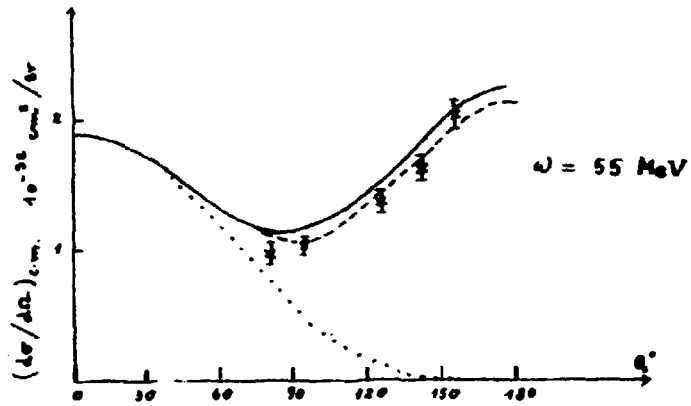

Fig.4.

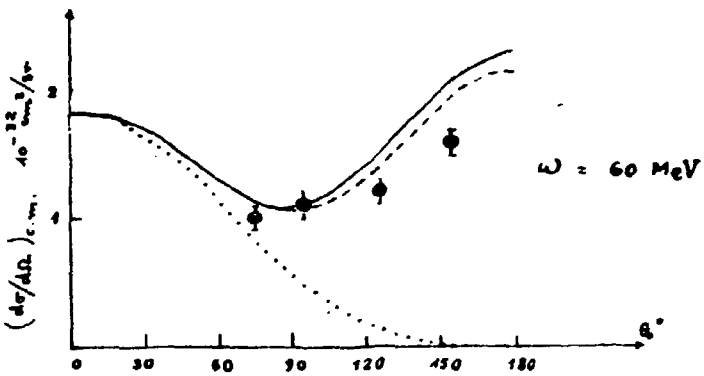

Fig.5.

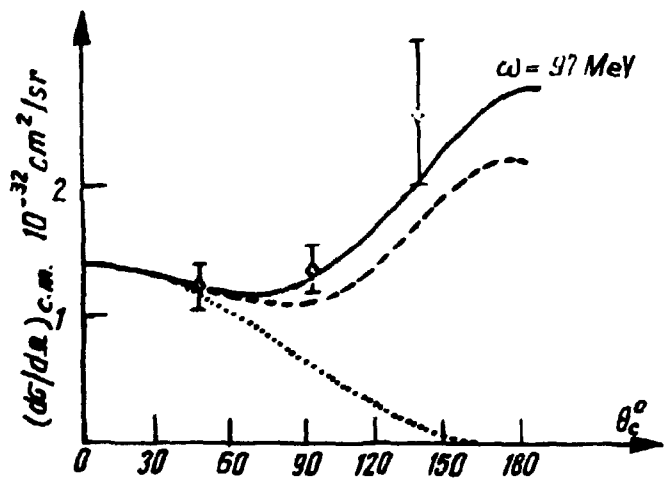

Fig.6.

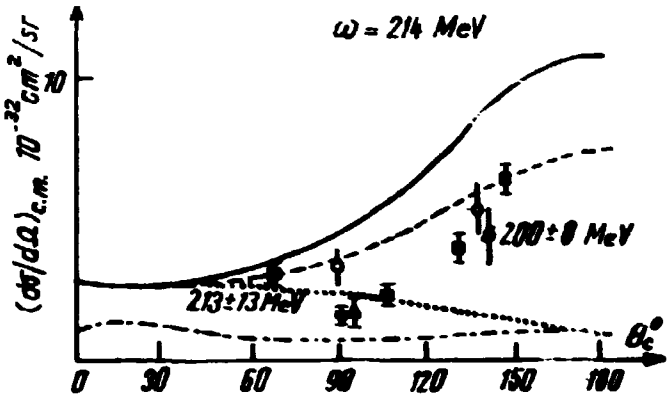

Fig. 7.

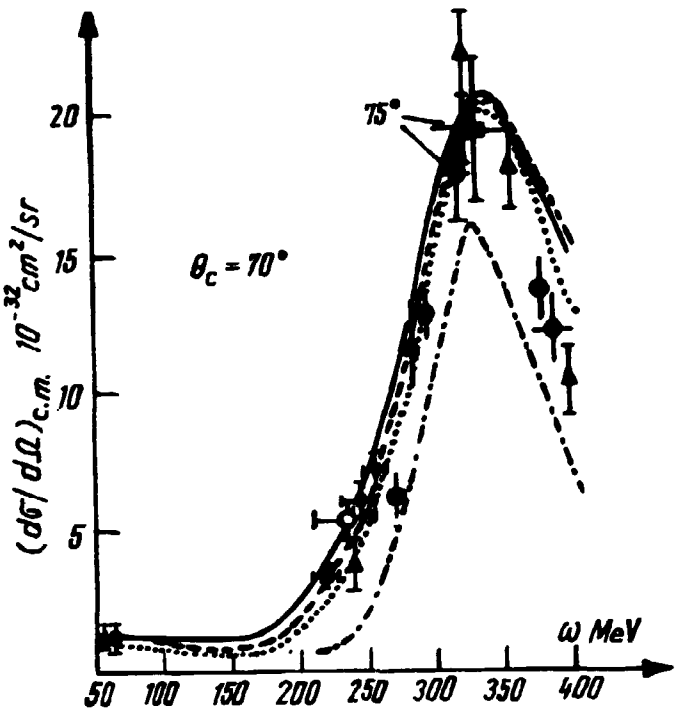

Fig. 8.

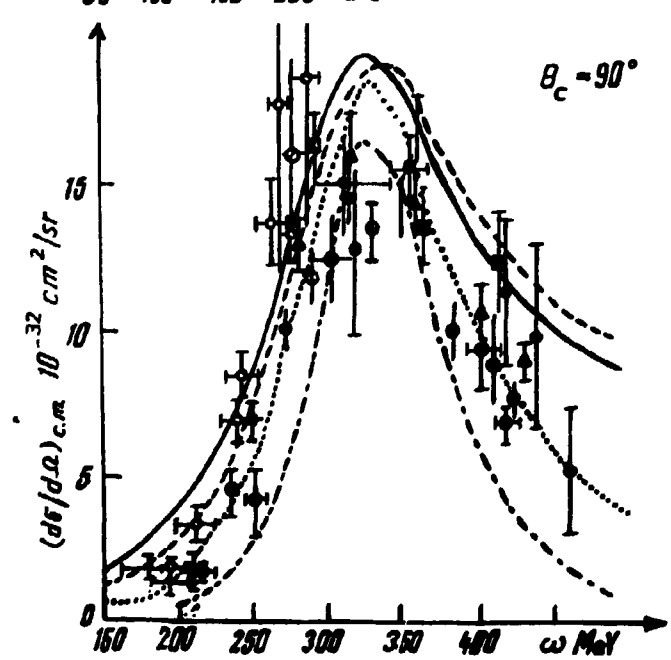

Fig. 9.

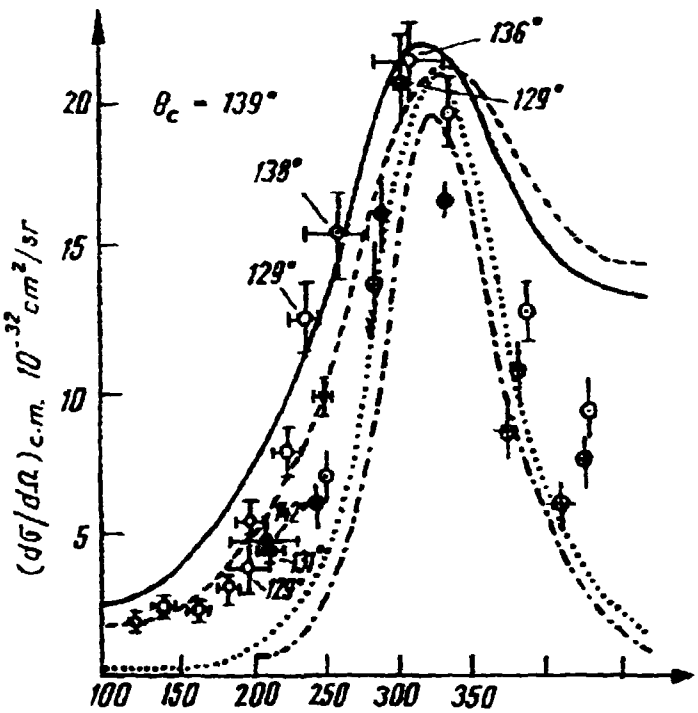
θ_c = 139°
136°
129°
138°
129°
125°
$(d\sigma/d\Omega)_{c.m.}$ 10^{-32} cm^2/sr
20
15
10
5
100
150
200
250
300
350

Fig. 10.

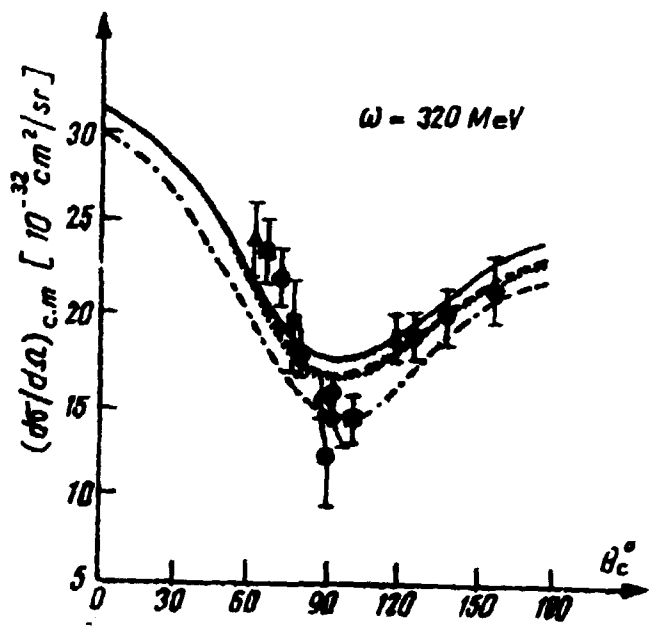
ω = 320 MeV
$(d\sigma/d\Omega)_{c.m}$ [10^{-32} cm^2/sr]
30
25
20
15
10
5
0
30
60
90
120
150
180
θ_c°

Fig. 11.

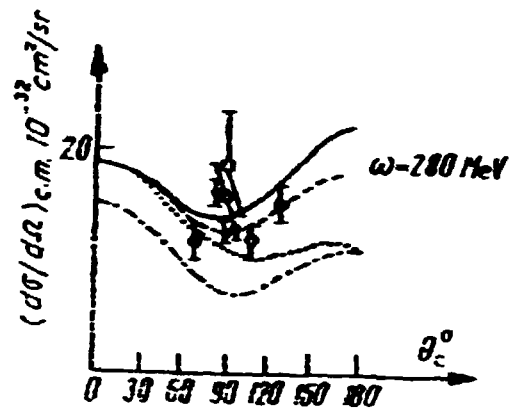

Fig. 12.

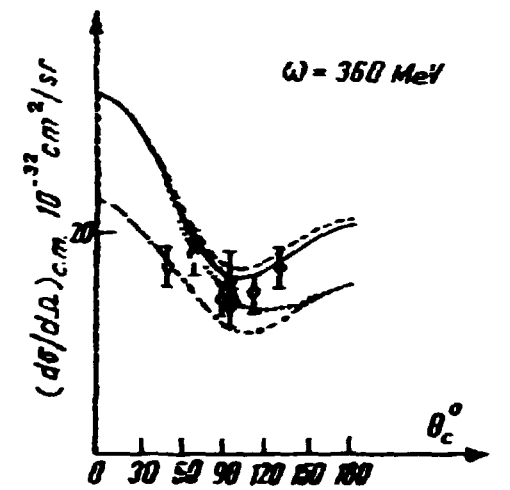

Fig. 13.

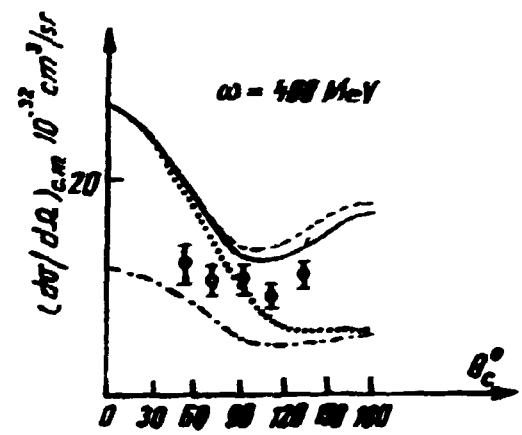

Fig. 14.

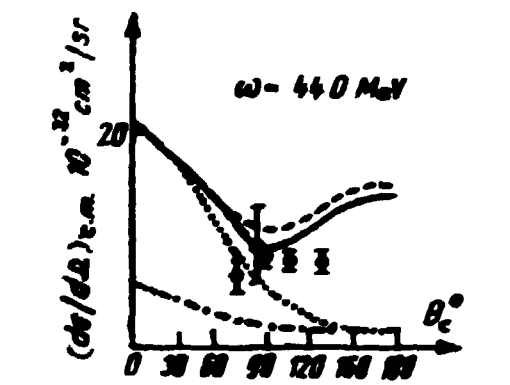

Fig. 15.